Hot Paper

Special Collection

Integrating Benzoxazine-PDMS 3D Networks with Carbon Nanotubes for flexible Pressure Sensors

Hugo Puozzo,[a, b] Shamil Saiev,[a] Leïla Bonnaud,*[b] David Beljonne,*[a] and Roberto Lazzaroni*[a]

Dedicated to Prof. Maurizio Prato on the occasion of his 70th birthday.

Shapeable and flexible pressure sensors with superior mechanical and electrical properties are of major interest as they can be employed in a wide range of applications. In this regard, elastomer-based composites incorporating carbon nanomaterials in the insulating matrix embody an appealing solution for designing flexible pressure sensors with specific properties. In this study, PDMS chains of different molecular weight were successfully functionalized with benzoxazine moieties in order to thermally cure them without adding a second component, nor a catalyst or an initiator. These precursors were then blended with 1 weight percent of multi-walled carbon nanotubes (CNTs) using an ultrasound probe, which induced a transition from a liquid-like to a gel-like behavior as CNTs generate an interconnected network within the matrix. After curing, the resulting nanocomposites exhibit mechanical and electrical properties making them highly promising materials for pressure-sensing applications.

Introduction

Pressure sensors are devices that can detect pressure by transforming it in a measurable electrical signal output.[1,2] This signal transduction operation makes it possible to exploit this type of devices in a wide variety of domains: automotive, medicine, industrial production, consumer goods and construction.[1,3–6] Conventional pressure sensors are made of inorganic materials that operate in rigid devices with limited flexibility and stretchability, as well as a low sensitivity.[5,7,8] Nowadays, the demand is growing to produce pressure sensors with increased mechanical and electrical properties to fulfill the requirements of the next-generation wearable devices, in terms of flexibility, stretchability, foldability, conformability, and sensitivity.[1,2,4] Many studies have been conducted on innovative ways to create flexible, stretchable, and sensitive force sensors.[9] Those sensors typically use conductive materials that are applied onto a flexible and stretchable polymeric substrate.[10–12] Those materials enable the sensors to function using various transduction mechanisms, including piezoresistive,[13,14] piezoelectric,[15,16] and capacitive[17,18] principles. Nanocomposite materials that are piezoresistive are of interest due to their high sensitivity, ease of manufacturing, simple read-out mechanism and low power consumption.[19] One particularly promising class of such materials is polymer nanocomposites that contain carbon nanomaterials such as graphene and carbon nanotubes (CNTs). They can be customized to meet specific application requirements and are expected to show superior sensitivity, chemical stability, mechanical and electrical properties.[20] In particular, polymer/CNTs composites reported in the literature often exhibit better electrical conductivity, strength, flexibility and stability than their counterparts with other types of nanofillers.[21–23]

Elastomers have been extensively used as flexible and stretchable insulating matrices coupled with a percolated network of CNTs for pressure-sensing composites.[1,24,25] These materials allow the sensor to be molded into different geometries, extending its range of applications.[5] The silicone rubber polydimethylsiloxane (PDMS) is the first choice as elastomeric matrix for the flexible electronic composites because of its low elastic modulus, inherent flexibility, high transparency, excellent chemical and thermal stability, and ease of use.[2,26–28] To become an elastomeric material, the initial PDMS has to be chemically cross-linked.[29,30] Various curing methods are known and commercialized to produce silicone resins:[31,32] (1) The cross-linking can be achieved by an addition reaction. It is performed by reacting vinyl-terminated polymers with SiH groups carried by functional oligomers. (2) A condensation reaction can also induce curing of a formulation

[a] Dr. H. Puozzo, Dr. S. Saiev, Prof. Dr. D. Beljonne, Prof. Dr. R. Lazzaroni
Laboratory for Chemistry of Novel Materials,
Materials Research Institute
University of Mons (UMONS)
20 Place du Parc, B-7000 Mons (Belgium)
E-mail: david.beljonne@umons.ac.be
        roberto.lazzaroni@umons.ac.be

[b] Dr. H. Puozzo, Dr. L. Bonnaud
Laboratory of Polymeric and Composite Materials (LPCM),
Center of Innovation and Research in Materials & Polymers (CIRMAP)
Materia Nova Research Center, Materials Research Institute
University of Mons (UMONS)
20 Place du Parc, B-7000 Mons (Belgium)
E-mail: s:
E-mail: Leila.Bonnaud@MATERIANOVA.be

Chemistry–A European Journal

Research Article
doi.org/10.1002/chem.202301791

Chemistry Europe
European Chemical
Societies Publishing

consisting of a hydroxy-terminated PDMS and a large excess of methyltriacetoxysilane. (3) Peroxide curing can also be employed. Organic peroxides are decomposed to form highly-reactive radicals that chemically cross-link the vinyl-containing PDMS chains. (4) Making the PDMS prepolymer sensitive to ultraviolet wavelengths is an alternative approach to PDMS processing.[33,34] The curing is then induced upon exposure to UV light. Even if these approaches work well and are used in large-scale production, they share some inherent drawbacks: they can leave by-products and often need a catalyst complex, an inhibitor and potentially specific reaction conditions.[35]

An alternative approach to cure PDMS polymers, while overcoming the shortcomings of other synthetic methods, is to functionalize the PDMS pre-polymer chain ends with benzoxazine moieties. Indeed, the oxazine rings can be used to generate cross-linking networks.[36] They are readily formed by a combination of a phenol, a primary amine, and formaldehyde in 1:1:2 molar ratio via a one-pot Mannich condensation. The synthesized compound then undergoes thermally-accelerated, cationic ring-opening polymerization without any additional initiator. Since the phenolic structure formed during the curing acts as an additional initiator and catalyst, the processing is autocatalyzed.[37] This class of thermosets are known to show good thermal and electrical features.[36–38]

Recently, we demonstrated experimentally[39–41] and theoretically[42,43] that benzoxazine resins facilitate the dispersion of CNTs without requiring a surface functionalizing agent, because of intrinsic favorable interactions between the two components. The use of a sonication probe can easily achieve a uniform dispersion state, resulting in nanocomposites with low electrical percolation thresholds, i.e., with amounts of CNTs as small as 0.5 wt%. This feature could therefore promote synergies with the high affinity of PDMS chains for adsorbing onto CNTs, which is driven by CH-π interactions between the methyl groups in the PDMS and the π-electron-rich surface of the CNTs.[44–46]

The addition of siloxane to benzoxazine moieties has been a popular option in the literature for improving the polybenzoxazine properties, including its ability to impart excellent flexibility and high thermal stability.[47–49] Various studies have integrated distinct siloxanes into benzoxazines, resulting in improved characteristics in the resulting polybenzoxazines, such as enhanced glass transition temperature (Tg) and toughness,[49–55] better thermal stability,[49,51—69] increased flame retardancy,[53,55,66,70] higher surface hydrophobicity,[71] improved mechanical properties,[51,58,62,64,72,73] enhanced shape memory effect,[48] corrosion resistance[74] and lower dielectric constant (low-k).[53,54,58,60,63,74,75] Particularly, Chou et al.[50] have been able to successfully synthesize a silicon-containing benzoxazine monomer prepared from 1,3-bis(3-aminopropyl)tetramethyldisiloxane (BATMS), phenol and formaldehyde aqueous solution for property modification on conventional phenol-based polybenzoxazines. Qi et al.[49] prepared the same monomer to incorporate it in a copolymer to significantly improve the toughness of the polybenzoxazines. Along the same line, our group[46] synthesized a benzoxazine-terminated polydimethylsiloxane (PDMS–Bz) from amino-terminated PDMS, paraformaldehyde and phenol to promote epoxy/PDMS compatibilization, as the benzoxazine moiety is reactive towards the epoxy system. In that case, the intended objective was to improve the thermal and flame-retardant properties of epoxy-based materials.
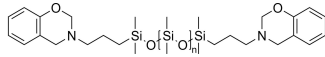
To the best of our knowledge, an elastomer including benzoxazine moieties was never used as the matrix for flexible pressure sensors. In this study, we explore more deeply the synthesis of PDMS–Bz (Table 1) by preparing three different polymers from aminopropyl-terminated PDMS of 1000 g.mol^{-1}, 2500 g.mol^{-1} and 5000 g.mol^{-1}. The thermal and mechanical properties of these three compounds are then fully characterized before and after addition of 1 wt% multi-walled carbon nanotubes in order to determine the effect of the filler.
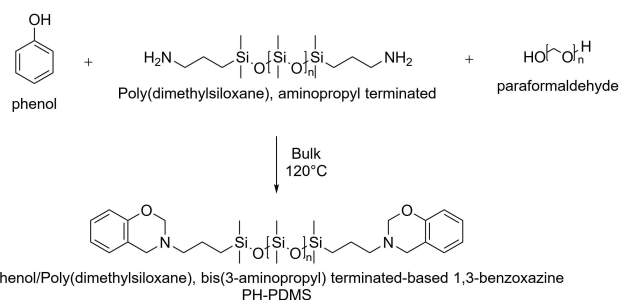
Results and Discussion

Structure of PH-PDMS

The three PH-PDMS benzoxazine compounds studied in this work were synthesized according to the one-pot Mannich condensation from phenol, bis(3-aminopropyl)-terminated poly(dimethylsiloxane), and paraformaldehyde in bulk, as shown in Scheme 1. To confirm the complete formation of the benzoxazine moieties at the chain end of the PDMS backbone, the ^{1}H NMR and ^{13}C NMR spectra of the PDMS-based benzoxazines of different molecular weights were recorded (Figure 1). In the ^{1}H NMR spectra, the characteristic proton resonance signals of the oxazine ring, assigned to the Ar-CH$_2$-N and O-CH$_2$-N protons, appear in all compounds as two singlets at 3.98 and 4.86 ppm, respectively. The resonant protons of the aminopropyl group are represented by peaks at 0.54, 1.58 and

Table 1. PH-PDMS benzoxazines synthesized.

Name	Chain Architecture
PH-PDMS structure	
	Molecular weight (g.mol^{-1})
PH-PDMS1000	~1250
PH-PDMS2500	~2750
PH-PDMS5000	~5250

Scheme 1. Synthesis of the PH-PDMS benzoxazine.

Chemistry–A European Journal

Research Article
doi.org/10.1002/chem.202301791

Chemistry Europe
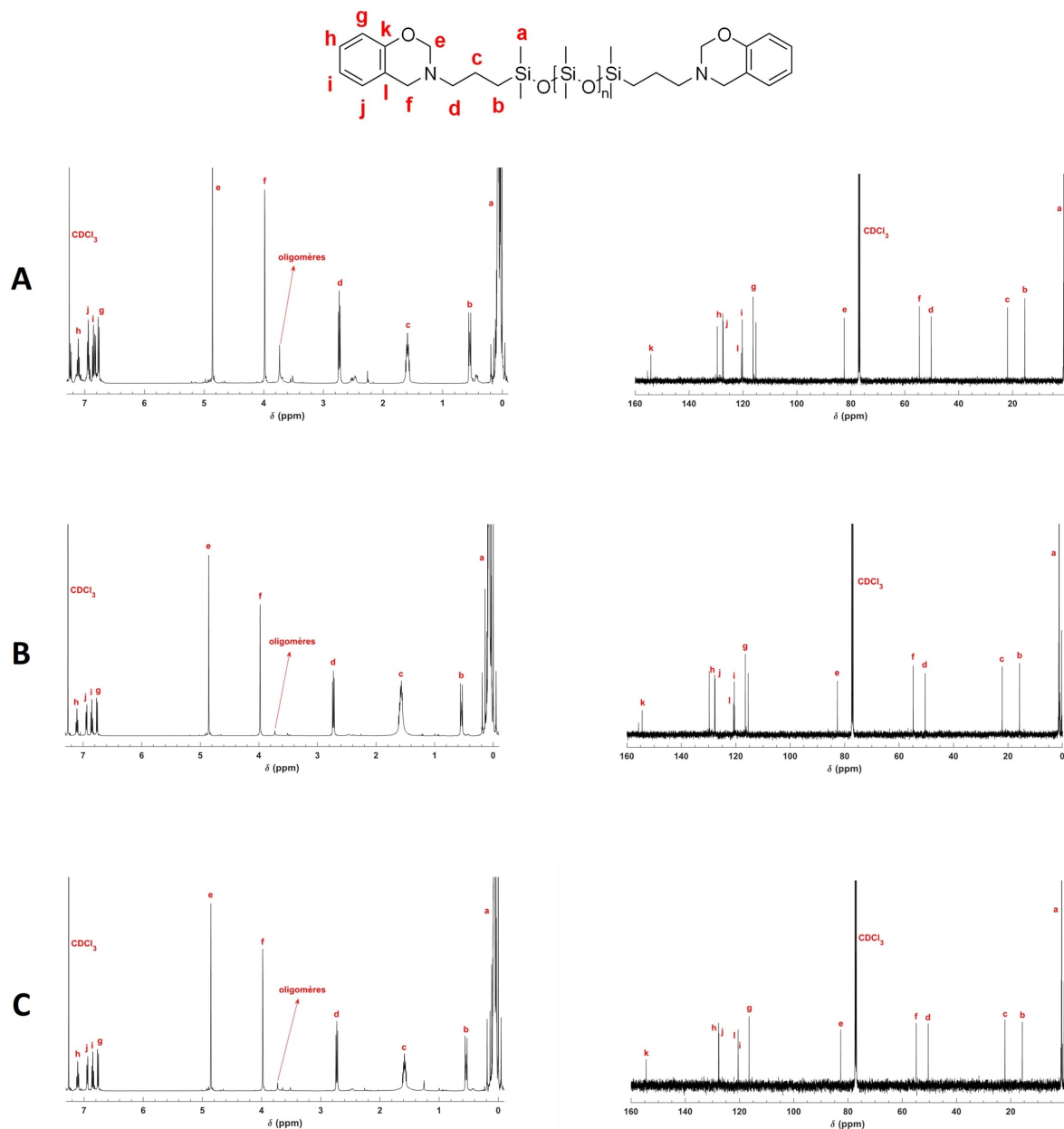European Chemical
Societies Publishing

Figure 1. The ^{1}H (left) and ^{13}C (right) NMR spectra of **(A)** PH-PDMS1000, **(B)** PH-PDMS2500, **(C)** PH-PDMS5000.

2.73 ppm.[49,51] The protons in the methyl groups of the PDMS chain correspond to the intense peak at 0.06-0.09 ppm. Based on our previous work on a trifunctional benzoxazine,[38] the peaks in the aromatic region between 6.74 and 7.14 ppm were unambiguously attributed to benzoxazine moieties also attached to the aminopropyl group, based on two-dimensional NMR analyses. It must be pointed out that some oligomers are inherently formed during the synthesis. The Mannich bridge protons of opened oxazine rings are typically located at approximately 3.70 ppm; the presence of proton peaks in this region thus indicates the formation of ring-opened oligomeric species from the monomers.[76]

In the ^{13}C NMR spectra of all the compounds, the signals at 54.8 and 82.7 ppm are the characteristic methylene carbon

resonances of Ar–$\underline{C}$H$_2$-N and O–$\underline{C}$H$_2$-N of the oxazine ring structure, respectively.[38,48,49] The peaks at 5.7, 22.1 and 50.5 ppm correspond to the resonant carbon of the amino-propyl group. The chemical shift at 1.2 ppm is assigned to the methyl groups of PDMS chain. Similar to the ^{1}H NMR, the aromatic carbon signals between 115.5 and 154.5 ppm can be assigned based on our previous work.[38]

The three PH-PDMS studied here were also analyzed by FTIR, shown in Figure 2. As expected, the characteristic signals of the PDMS chain increase with the molecular weight at the expense of the characteristic peaks of the benzoxazine moieties, which are almost undetectable for PH-PDMS5000. For all the samples, the PDMS absorptions appear at about 787 cm^{-1} for the stretching vibrations of the Si-C,[49] 1015 cm^{-1} for the
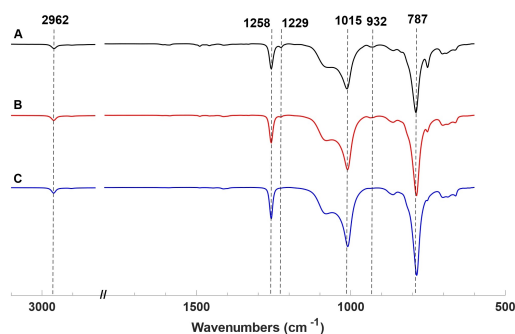
Chem. Eur. J. **2023**, e202301791 (3 of 11)

© 2023 Wiley-VCH GmbH

Chemistry–A European Journal

Research Article
doi.org/10.1002/chem.202301791

Chemistry Europe
European Chemical
Societies Publishing

Figure 2. FTIR spectra of the uncured (**A**) PH-PDMS1000, (**B**) PH-PDMS2500, (**C**) PH-PDMS5000.

asymmetric stretching vibrations of Si–O–Si,[77] 1258 cm^{-1} for the Si-CH$_3$ bending vibration and 2962 cm^{-1} for the C–H symmetric stretching vibrations of CH$_3$.[48] Regarding the benzoxazine parts, we can detect the C–O–C asymmetric stretching mode at about 1229 cm^{-1} and the band at 932 cm^{-1} characteristic of the oxazine ring mode.[38,78] It must be pointed out that the C–O-C symmetric stretching mode at 1033 cm^{-1} as well as the =C–H stretching vibrations of the aromatic ring at 3040 cm^{-1} and the C–H symmetric stretching vibrations of CH$_2$ propyl chains at about 2860 cm^{-1} are masked by the other peaks.
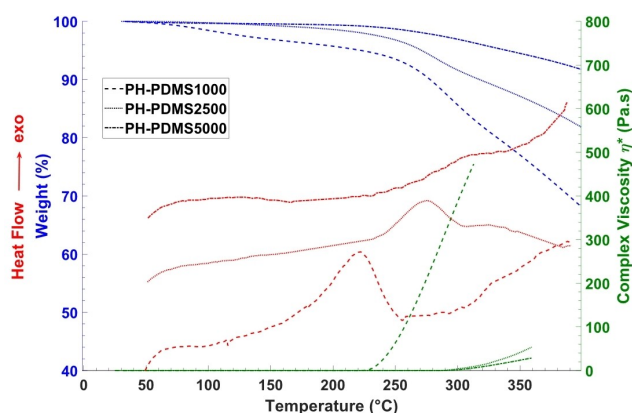

Figure 3. DSC (red), TGA (blue) and viscosity (green)-temperature curves of PH-PDMS1000, PH-PDMS2500 and PH-PDMS5000.

Polymerization of PH-PDMS

The three precursors (PH-PDMS1000, PH-PDMS2500, and PH-PDMS5000) were subjected to Differential Scanning Calorimetry (DSC), Thermogravimetric Analysis (TGA), and Dynamic Rheological Analysis (DRA) measurements to track structural changes with temperature, reactivity, and thermal stability. These results are collected in Figure 3, and the important values are listed in Table 2. The DSC exothermic peak maximum, which corresponds to resin curing (the schematic network is presented in Scheme 2), coincides with the onset of the increase in complex viscosity η* obtained by DRA, as typically observed in the cross-linking of Bz compounds;[38,79,80] in a control experiment, we have checked that a similar heat treatment applied to non-functionalized PDMS yields no solid material. Notably, the onset, maximum, and enthalpy of the exotherm as well as the temperature corresponding to the increase in η* all rise with the PDMS chain molecular weight, which is attributed to the dilution effect:[81,82] the benzoxazine moieties are increasingly diluted by PDMS, which raises the benzoxazine ring-opening temperature. The initial degradation step detected by TGA above 250 °C, which has been linked to the volatilization of imine products as a result of secondary rearrangement reactions connected to the curing process,[79,83] takes place in the same range as the exothermic peak and the rise in η*, suggesting that the degradation process starts in the final stages of the polymerization of the precursors. However, it seems that the small weight losses during curing do not significantly affect the PH-PDMS ability to cure, as bulk materials could be produced without any issues. Thus, the PH-PDMS precursors can be simply heated to be cured without the use of a catalyst or initiator.

Addition of multi-walled carbon nanotubes and characterization of the uncured blends

After the synthesis and characterization of the PH-PDMS precursors, their mixtures with 1 weight percent of CNTs were prepared. To fully exploit the extraordinary capabilities of CNTs in a polymer composite, it is well recognized that the degree of dispersion within the polymer matrix is of utmost importance.[39,41,84] A rheological method was used before

Table 2. Thermal properties of PH-PDMS1000, PH-PDMS2500 and PH-PDMS5000 as determined by DSC, TGA and DRA.

Sample	Tp$_{onset}$ from DSC[a] (°C)	Tp$_{max}$[b] (°C)	Enthalpy[c] (J.g^{-1})	Weight loss at Tp$_{onset}$ from DSC[d] (%)	Weight loss at Tp$_{max}$[e] (%)	Tp$_{onset}$ from η*[f] (Pa.s)	Weight loss at Tp$_{onset}$ from η*[g] (%)
PH-PDMS1000	178	223	33.6	4	5	222	5
PH-PDMS2500	240	277	13.0	3	6	288	7
PH-PDMS5000	267	304	5.1	2	3	291	3

[a] Onset temperature of the reaction exotherm as obtained by DSC. [b] Maximum temperature of the reaction exotherm as obtained by DSC. [c] Reaction enthalpy as obtained by DSC. [d] Weight loss at the onset temperature of the exotherm as obtained by TGA-N$_2$. [e] Weight loss at the maximum temperature of the exotherm as obtained by TGA-N$_2$. [f] Onset temperature of the increase of the complex viscosity η* as obtained by DRA. [g] Weight loss at the onset temperature of the increase of the complex viscosity η* from the viscosity–temperature curve as obtained by TGA-N$_2$.

Chem. Eur. J. **2023**, e202301791 (4 of 11)

© 2023 Wiley-VCH GmbH
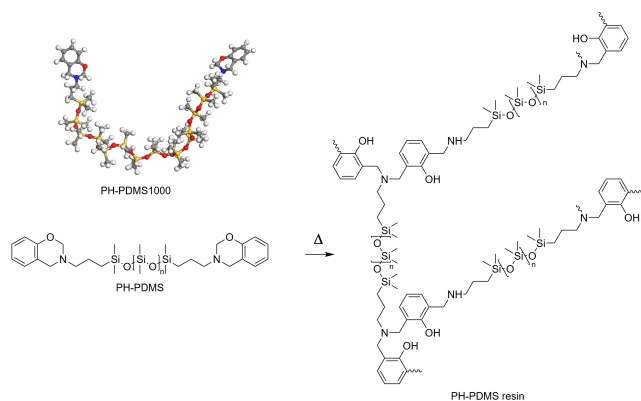
Scheme 2. Schematic representation of the network formed upon polymerization of PH-PDMS.

curing, as this approach is efficient to characterize the confinement and the dispersion of particles within a polymer matrix.[39,85] The amplitude sweeps on the three PH-PDMS precursors without CNTs in Figure 4 reveal that the storage (G′) modulus (elastic properties) is smaller than the loss (G″) modulus (viscous properties) in the linear viscoelastic regime, indicating a fluid behavior. When the filler is added to the PH-PDMS, the two moduli strongly increase and G′ now exceeds G″, which is characteristic of a gel-like behavior and is significant of the presence of good interactions between CNTs and PH-PDMS chains. Indeed, when particle/matrix interactions are favored in liquid polymers, CNTs can therefore disentangle, separate from each other, disperse, reorganize themselves and create an interconnected network. This structural network is

responsible for the enhancement of G′ and G″ and for their independence versus the shear strain in the low shear strain range, manifesting as a plateau in Figure 4.

The frequency sweeps performed on the PH-PDMS precursors and their nanocomposites with CNTs are presented in the Figure S1 (Supporting Information). Based on the prior amplitude sweeps, the applied shear strain was selected to be in the linear viscoelastic zone. The same conclusions can be deduced from these experiments: samples without filler exhibit a viscoelastic liquid-like behavior and adding CNTs imparts a solid-like behavior to the blends, significantly increasing G′ and G″ and making them frequency-independent in all the probed range, indicating good interactions between CNTs and PH-PDMS matrix.

Molecular dynamics (MD) simulations have been employed to provide a detailed understanding of the interfacial interactions between uncured PH-PDMS polymer chains and carbon nanotubes. As the experimental CNT diameter of approximately 9.5 nm exceeds the atomistic limits of the MD simulations, to simplify the model, a graphene sheet was substituted for the CNT, serving as a representative local region of the nanotube. On the length scale of the MD simulation box, the outer surface of a 10-nm diameter MWCNT is virtually flat and our previous studies[42,43] have shown that considering multi-layer graphene instead of a single layer to represent the carbon surface does not modify significantly the nature and strength of the interactions with the resin, hence the use of a single graphene sheet here. Simulation boxes, containing periodic 9.4×9.4 nm^2 graphene sheets, were loaded with 350 and 100, PH-PDMS1000 and PH-PDMS5000 polymer chains, respectively. These resulting structures were then equilibrated at room temperature and
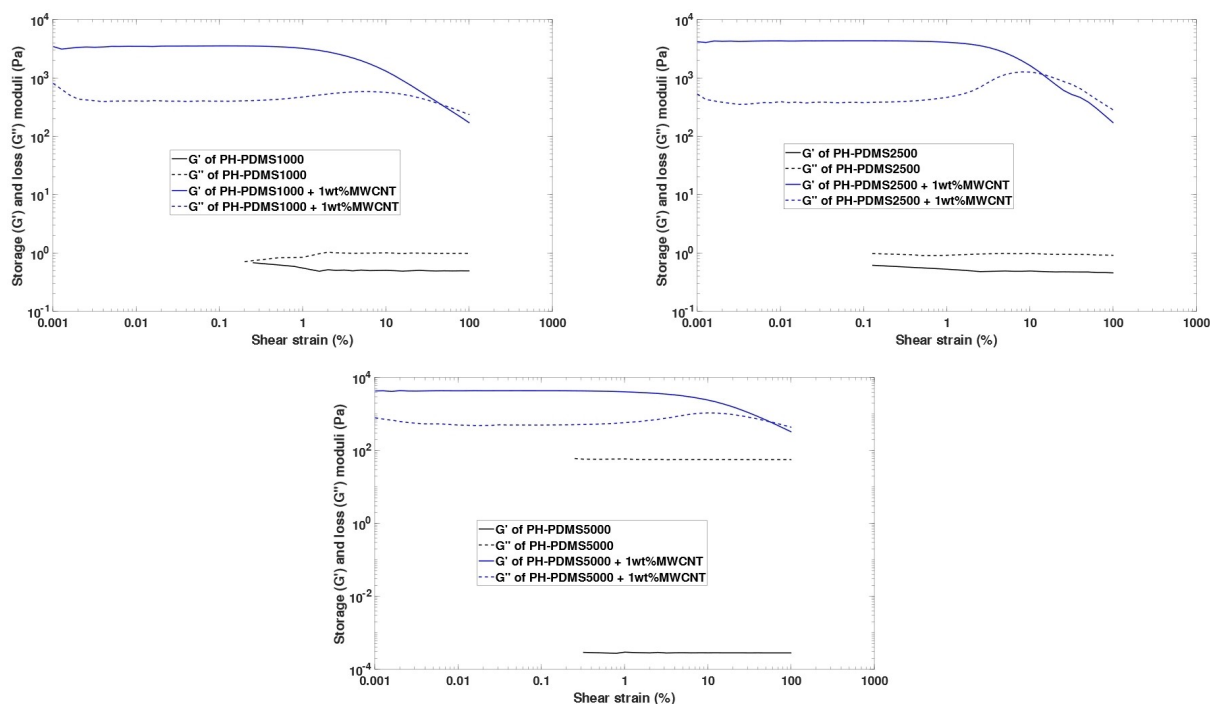

Figure 4. DRA curves (amplitude sweep, frequency = 1 Hz at room temperature) of the uncured PH-PDMS1000, PH-PDMS2500 and PH-PDMS5000 and their mixtures with 1 wt% MWCNTs.
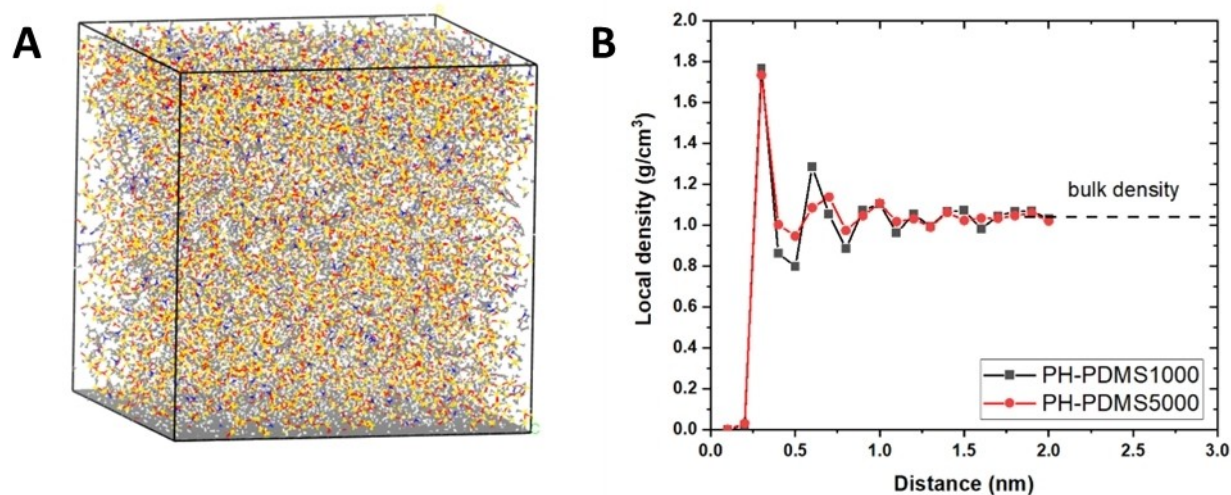
Chem. Eur. J. **2023**, e202301791 (5 of 11)

© 2023 Wiley-VCH GmbH

Chemistry–A European Journal

Research Article
doi.org/10.1002/chem.202301791

Chemistry Europe
European Chemical
Societies Publishing

Figure 5. (**A**) Snapshot from the MD simulations illustrating the PH-PDMS/graphene interface; silicon: yellow; oxygen: red; nitrogen: blue; carbon: grey. (**B**) Local density of PH-PDMS1000 and PH-PDMS5000 structures, varying with the distance from the graphene sheet.

atmospheric pressure under the NPT ensemble (Figure 5.A). The simulations revealed a specific interfacial arrangement of the PH-PDMS polymer chains relative to the graphene surface. This can be elucidated via local density profiles as a function of the distance from the graphene layer. As shown in Figure 5.B, a dense interface region approximately 2 nm thick is formed, with the highest peaks representing the primary layer of chains adhering to the surface due to strong π-π and CH-π interactions.

To evaluate the interfacial energy E_{int}, we carried out three separate simulations to determine the different terms in the equation $E_{int} = E_{PH-PDMS/graphene} - E_{PH-PDMS} - E_{graphene}$. These simulations involved equilibrating PH-PDMS/graphene, bulk PH-PDMS, and bulk graphene structures. Additionally, we computed the density of π-π interactions between graphene and benzoxazine moieties, as they are expected to contribute markedly to the matrix/CNT interactions. The results indicate a favorable interfacial energy for both systems, with values of 305.1 mJ.m^{-2} for PH-PDMS1000 and 281.6 mJ.m^{-2} for PH-PDMS5000. The slightly higher interfacial energy for PH-PDMS1000 can be attributed to a higher density of π-π interactions (0.78 π-π/nm^2) compared to PH-PDMS5000 (0.35 π-π/nm^2), which aligns with earlier findings.[42] These results rationalize the favorable distribution of CNTs in the PH-PDMS matrices, which we observe experimentally.

Curing of the PH-PDMS resins and their nanocomposites

Cross-linked polybenzoxazine networks were prepared by curing the PH-PDMS precursors and their nanocomposites with 1 wt% MWCNTs according to the conditions described in the Experimental Section.

Conventional DSC measurements failed to identify the glass transition temperature Tg of the cured materials. Thus, thermomechanical analysis was used to determine the mechanical transition temperature Tα associated with the Tg. Since the

ultimate goal is to fabricate a matrix for flexible pressure sensors, dynamic mechanical analysis (DMA) was used in compression mode to determine the properties of the materials in the final state after curing. The results are shown in Figure 6 and the important values are summarized in Table 3. Concerning the pristine resins, it appears that the Tg of the material decreases with the molecular weight of the PH-PDMS, which is associated with a higher segmental mobility between crosslinks. Concomitantly, the height of the tan δ peak, which is linked to the cross-link density, increases. Since tan δ is the ratio of the viscous to elastic response of a viscoelastic material, this increasing height is associated with a higher segmental mobility and thus indicates of a lower degree of cross-linking.[86] This is confirmed by the lower value of the storage modulus in the rubbery area.

When PH-PDMS is filled with 1 wt% CNTs, no significant change of Tg or height of the tan δ peak is observed. Only a slight increase is obtained for the rubbery plateau. These results suggest that CNTs alter only slightly the mobility of the chains between cross-links.

Table 3. Thermomechanical properties of the cured PH-PDMS1000, PH-PDMS2500 and PH-PDMS5000 resins and their nanocomposites with 1 wt% MWCNTs as obtained by DMA.

Sample	Tα[a] (°C)	E$^{r[b]}$ at 25 °C (MPa)
PH-PDMS1000	−97	0.561
PH-PDMS1000 + 1wt%MWCNT	−92	0.861
PH-PDMS2500	−101	0.015
PH-PDMS2500 + 1wt%MWCNT	−105	0.024
PH-PDMS5000	−107	0.007
PH-PDMS5000 + 1wt%MWCNT	−104	0.054

[a] Temperature of maximum tan δ peak as obtained by DMA. [b] Storage modulus at 25 °C as obtained by DMA.
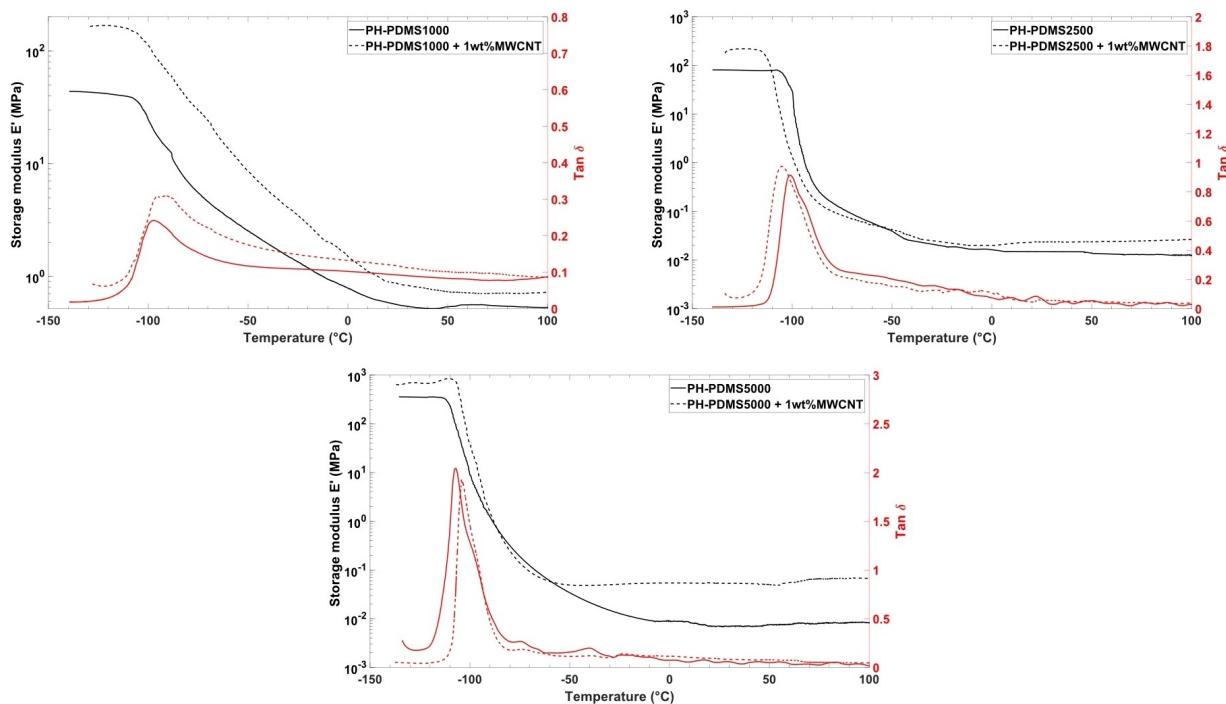
Chemistry–A European Journal

Research Article
doi.org/10.1002/chem.202301791

Chemistry Europe
European Chemical
Societies Publishing

Figure 6. DMA thermograms (temperature sweep, frequency = 1 Hz, and ramp rate = 3 °C.min^{-1}) of the cured PH-PDMS1000, PH-PDMS2500 and PH-PDMS5000 resins and their nanocomposites with 1 wt% MWCNT.

Overall, it appears that the presence of MWCNTs still allows molecular chain mobility in the rubbery state; this makes it possible to generate nanocomposites with high flexibility at room temperature, which is ideal for flexible pressure sensors.

The cured materials were tested by DRA in the oscillatory shear mode. A strain amplitude sweep test at room temperature and 1 Hz was first performed (Figure 7). The shear resistance of the materials at room temperature can thus be determined by
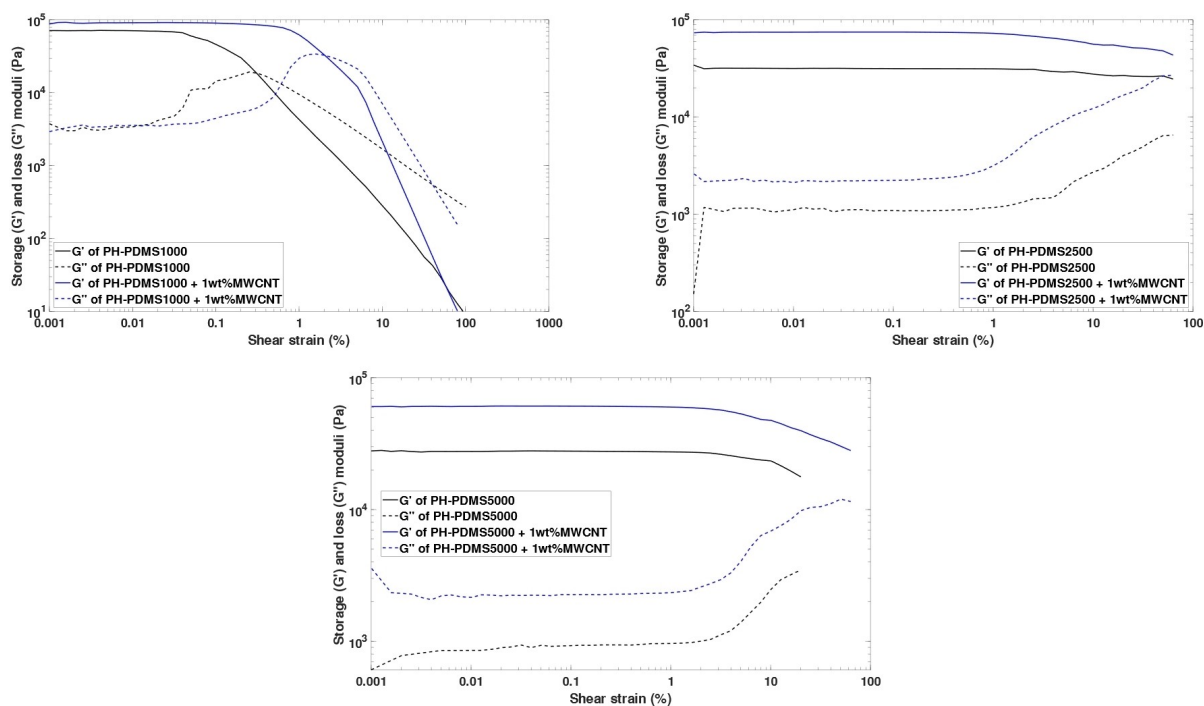

Figure 7. DRA curves (amplitude sweep, frequency = 1 Hz at room temperature) of the cured PH-PDMS1000, PH-PDMS2500 and PH-PDMS5000 resins and their nanocomposites with 1 wt% MWCNTs.

Chemistry–A European Journal

Research Article
doi.org/10.1002/chem.202301791

Chemistry Europe
European Chemical
Societies Publishing

these experiments. The storage (G') shear modulus at the zero-strain limit decreases with the molecular weight of the PH-PDMS. Also, G' of PH-PDMS2500, PH-PDMS5000 and their nanocomposites remains constant over a larger shear strain range compared to the PH-PDMS1000 and its nanocomposite, which emphasizes that they are softer materials that can withstand larger deformation. The G' value in shear mode increases with the filler, which is attributed to the cluster-free and uniform dispersion of CNTs that leads to a slight decrease of the molecular chain mobility.[87]

The frequency sweep at shear strain $=0.01\%$ and room temperature of the material shows that G' is frequency independent in all the probed angular frequency ω in shear mode. This confirms the results obtained by strain amplitude sweep test. The details of these data are presented in the Figure S2 (Supporting Information).

As already observed for PDMS,[88] the overall picture from the mechanical measurements is that the addition of MWCNTs into the PH-PDMS matrix does not affect drastically the viscoelastic behavior of PH-PDMS in compression (as obtained by DMA) and under shear (as obtained by DRA).

Electrical measurements were finally performed on the various materials to detect the formation of electrical percolation paths of the CNTs within the PH-PDMS matrix by the increase of the conductivity σ. Table 4 shows the electrical data obtained for the different PH-PDMS and their nanocomposites with 1 wt% MWCNTs. Remarkably, the conductivity is improved by a factor 10^5-10^6 when the CNTs are added in the matrix. These values are in the same range as the nanocomposites of PDMS/1 wt% MWCNTs[89–91] and polybenzoxazine/1 wt% MWCNTs[39,41] reported in the literature.

This strong increase in the conductivity confirms the results reported above regarding the formation of a network-like structure of the CNTs in the nanocomposites observed by DRA analyses, giving rise to electrical percolation paths within the material.

Conclusions

Benzoxazine-terminated PDMS polymers (PH-PDMS) of three different molecular weights were successfully synthesized from bis(3-aminopropyl)-terminated poly(dimethylsiloxane), phenol and paraformaldehyde. Their thermal curing shows that the resins can be obtained without the use of any initiator or catalyst, contrary to the conventional PDMS for which a hardener or a catalyst is needed.

Adding 1%wt CNTs leads to an interconnected network within the PH-PDMS matrices, which induces the transition from a liquid-like to a gel-like behavior for the blend and a major increase in the storage shear modulus. This reflects the good dispersion of CNTs within the PH-PDMS matrices, which is spurred by favorable interfacial interactions identified with MD simulations.

Thermomechanical analysis of the cured resins shows that the Tg and the cross-linking density are only slightly affected by the presence of 1 wt% CNTs, highlighting that the PH-PDMS based nanocomposites have elastomer properties. This behaviour is further confirmed with amplitude and frequency sweeps analyses by shear mode in DRA at room temperature.

Finally, electrical measurements confirm that a network-like structure is formed by the CNTs within the matrix, which drastically improves the electrical conductivity of the resin.

These results show that the conventional PDMS can be thermally cured to generate an elastomer, without the use of an additional component when it is end-functionalized with benzoxazine moieties. The systems developed here do not require either any surface treatment or functionalization of the CNTs to promote their dispersion within the matrix, which makes them promising for pressure-sensing applications.

Experimental Section

Materials

Poly(dimethylsiloxane), bis(3-aminopropyl) terminated (1000 g.mol^{-1} and 5000 g.mol^{-1}) were purchased from ABCR whereas the 2500 g.mol^{-1} polymer was acquired from Sigma-Aldrich. Phenol ($>99\%$) was obtained from Merckmillipore. Paraformaldehyde ($>99\%$), diethylether and chloroform were used as received from VWR. Multi-walled carbon nanotubes (MWCNTs - NC7000™, diameter of ~9.5 nm and an average length of ~1.5 μm) were purchased from Nanocyl.

Preparation of Benzoxazine-Terminated poly(dimethylsiloxane) 100 preparation of Benzoxazine-Terminated poly(dimethylsloxane) 1000 g mol^{-1} (PH-PDMS1000)

Phenol (1.02 g, 0.011 mol) and paraformaldehyde in excess (0.72 g, 0.024 mol) were introduced into a 50 mL round-bottom flask and immersed in an oil bath preheated at 120°C. The mixture was

Table 4. Electrical properties of the cured PH-PDMS1000, PH-PDMS2500 and PH-PDMS5000 resins and their nanocomposites with 1 wt% MWCNTs.

Sample	Conductivity σ (S/m)
PH-PDMS1000	1.85×10^{-10}
PH-PDMS1000 + 1 wt% MWCNT	6.38×10^{-5}
PH-PDMS2500	2.26×10^{-10}
PH-PDMS2500 + 1 wt% MWCNT	1.11×10^{-4}
PH-PDMS5000	4.35×10^{-10}
PH-PDMS5000 + 1 wt% MWCNT	3.29×10^{-5}

Chem. Eur. J. **2023**, e202301791 (8 of 11)

© 2023 Wiley-VCH GmbH

Chemistry–A European Journal

Research Article
doi.org/10.1002/chem.202301791

Chemistry Europe
European Chemical
Societies Publishing

stirred until the complete melting of phenol and the subsequent formation of a homogenous white solution. Poly(dimethylsiloxane), bis(3-aminopropyl) terminated 1000 g.mol^{-1} (4.9 g, 5.44×10^{-3} mol) was then added into the mixture. The addition of the diamine leads to the gelation of the mixture resulting from the condensation of the diamine and formaldehyde and the subsequent formation of a triazine network.[92] At this temperature, the triaza compound reacts quickly with phenol and the gel is disrupted in 2 min. The mixture was then allowed to react 10 min under continuous stirring. After cooling to room temperature, the reaction mixture was then dissolved in ET$_2$O, filtered by Büchner, and dried under vacuum to obtain PH-PDMS1000 as a transparent viscous liquid. ^{1}H NMR (500 MHz, CDCl$_3$, 25 °C, TMS): δ = 7.11 (m, 2H; Ar–H), 6.99–6.91 (m, 2H; Ar–H), 6.89–6.80 (m, 2H; Ar–H), 6.77 (m, 2H; Ar–H), 4.86 (s, 4H; O-CH$_2$-N), 3.98 (s, 4H; Ar-CH$_2$-N), 2.77–2.70 (t, 4H; N-CH$_2$), 1.64–1.54 (tt, 4H; CH$_2$), 0.58–0.51 (t, 4H; CH$_2$-Si), 0.08 (s; Si-CH$_3$). ^{13}C NMR (126 MHz, CDCl$_3$, 25 °C, TMS): δ = 154.19 (O–Ar), 127.51 (Ar), 127.39 (Ar), 120.32 (Ar), 120.23 (CH$_2$-C), 116.27 (Ar), 82.44 (O-CH$_2$-N), 54.57 (N-CH$_2$-Ar), 50.17 (N-CH$_2$), 21.87 (CH$_2$), 15.46 (Si-CH$_2$), 1.23 (Si-CH$_3$). FTIR (cm^{-1}): $\tilde{\nu}$ = 2962 (m) (C–H symmetric stretching of CH$_3$), 1258 (s) (bending of Si–CH$_3$), 1229 (w) (asymmetric stretching of C–O–C), 1015 (s) (asymmetric stretching of Si–O–Si), 932 (w) (oxazine ring mode), 787 (vs) (stretching of Si–C).

Preparation of Benzoxazine-Terminated Poly(dimethylsiloxane) 2500 g mol^{-1} (PH-PDMS2500)

Phenol (0.37 g, 3.92×10^{-3} mol) and paraformaldehyde in excess (0.26 g, 8.92×10^{-3} mol) were introduced into a 50 mL round-bottom flask and immersed in an oil bath preheated at 120 °C. The blend was stirred until the complete melting of phenol and the subsequent formation of a homogenous white solution. Poly(dimethylsiloxane), bis(3-aminopropyl)-terminated 2500 g.mol^{-1} (4.9 g, 1.96×10^{-3} mol) was then added into the mixture. The addition of the diamine leads to the gelation of the mixture resulting from the condensation of the diamine and formaldehyde and the subsequent formation of a triazine network.[92] At this temperature, the triaza compound reacts quickly with phenol and the gel is disrupted in 5 min. The mixture was then allowed to react 60 min under continuous stirring. After cooling to room temperature, the reaction mixture was then dissolved in ET$_2$O, filtered by Büchner, and dried under vacuum to obtain PH-PDMS2500 as a transparent viscous liquid. ^{1}H NMR (500 MHz, CDCl$_3$, 25 °C, TMS): δ = 7.18–7.05 (m, 2H; Ar–H), 7.00–6.89 (m, 2H, Ar–H), 6.89–6.80 (m, 2H; Ar–H), 6.77 (m, 2H; Ar–H), 4.86 (s, 4H; O-CH$_2$-N), 3.98 (s, 4H; Ar-CH$_2$-N), 2.77–2.70 (t, 4H; N-CH$_2$), 1.64–1.53 (tt, 4H; CH$_2$), 0.58–0.51 (t, 4H; CH$_2$-Si), 0.16–0.04 (s; Si-CH$_3$). ^{13}C NMR (126 MHz, CDCl$_3$, 25 °C, TMS): δ = 154.43 (O–Ar), 127.77 (Ar), 127.65 (Ar), 120.57 (Ar), 120.48 (CH$_2$-C), 116.52 (Ar), 82.69 (O-CH$_2$-N), 54.82 (N-CH$_2$-Ar), 50.42 (N-CH$_2$), 22.12 (CH$_2$), 15.72 (Si-CH$_2$), 1.22 (Si-CH$_3$). FTIR (cm^{-1}): $\tilde{\nu}$ = 2962 (m) (C–H symmetric stretching of CH$_3$), 1258 (s) (bending of Si-CH$_3$), 1229 (w) (asymmetric stretching of C–O–C), 1015 (s) (asymmetric stretching of Si–O–Si), 932 (w) (oxazine ring mode), 787 (vs) (stretching of Si–C).

Preparation of Benzoxazine-Terminated Poly(dimethylsiloxane) 5000 g mol^{-1} (PH-PDMS5000)

Phenol (0.18 g, 1.96×10^{-3} mol) and paraformaldehyde in excess (0.13 g, 4.31×10^{-3} mol) were introduced into a 50 mL round-bottom flask and immersed in an oil bath preheated at 120 °C. The blend was stirred until the complete melting of phenol and the subsequent formation of a homogenous white solution. Poly(dimethylsiloxane), bis(3-aminopropyl) terminated 5000 g.mol^{-1} (4.9 g, 9.8×10^{-4} mol) was then added into the mixture. The addition

of the diamine leads to the gelation of the mixture resulting from the condensation of the diamine and formaldehyde and the subsequent formation of a triazine network.[92] At this temperature, the triaza compound reacts quickly with phenol and the gel is disrupted in 10 min. The mixture was then allowed to react 60 min under continuous stirring. After cooling to room temperature, the reaction mixture was then dissolved in ET$_2$O, filtered by Büchner, and dried under vacuum to obtain PH-PDMS5000 as a transparent viscous liquid. ^{1}H NMR (500 MHz, CDCl$_3$, 25 °C, TMS): δ = 7.11 (m, 2H; Ar–H), 6.94 (m, 2H; Ar–H), 6.85 (m, 2H; Ar–H), 6.76 (m, 2H; Ar–H), 4.86 (s, 4H; O-CH$_2$-N), 3.98 (s, 4H; Ar-CH$_2$-N), 2.77–2.68 (t, 4H; N-CH$_2$), 1.58 (tt, 4H; CH$_2$), 0.59–0.50 (t, 4H; CH$_2$-Si), 0.16–0.02 (s; Si-CH$_3$). ^{13}C NMR (126 MHz, CDCl$_3$, 25 °C, TMS): δ = 154.46 (O–Ar), 127.76 (Ar), 127.65 (Ar), 120.56 (Ar), 120.50 (CH$_2$-C), 116.52 (Ar), 82.72 (O-CH$_2$-N), 54.83 (N-CH$_2$-Ar), 50.43 (CH$_2$), 15.72 (Si-CH$_2$), 1.22 (Si-CH$_3$). FTIR (cm^{-1}): $\tilde{\nu}$ = 2962 (m) (C–H symmetric stretching of CH$_3$), 1258 (s) (bending of Si-CH$_3$), 1229 (w) (asymmetric stretching of C–O–C), 1015 (s) (asymmetric stretching of Si–O–Si), 932 (w) (oxazine ring mode), 787 (vs) (stretching of Si–C).

General Formulation of PH-PDMS + 1 wt % CNTS

PH-PDMS and CNTs (1%wt) were mixed in chloroform at room temperature and sonicated via ultra-sound probe in a pulse mode for 1 min. The solvent was then evaporated to give a black soft solid.

Curing of PH-PDMS and PH-PDMS + 1 wt % CNTS

The PH-PDMS polymers as well as their mixture with CNTs were cured at 140 °C, 160 °C, 180 °C, 200 °C, 220 °C and 230 °C for 1 h at each temperature, respectively.

Characterization

1D ^{1}H and ^{13}C NMR spectra were recorded on a Bruker AMX-500 (500 MHz) NMR spectrometer in chloroform-d (CDCl$_3$) with TMS as an internal standard. Fourier Transform Infrared (FTIR) spectra were obtained using a Bruker Tensor 17 FTIR spectrometer, operating in ATR-FTIR («Attenuated Total Reflectance-Fourier Transform Infra-Red») mode. Differential Scanning Calorimetry (DSC) data were obtained from a DSC 2920 apparatus (TA Instruments) at a heating rate of 10 °C.min^{-1} in a nitrogen flow (88 mL.min^{-1}) for all tests. Thermogravimetric Analyses (TGA) were performed on a TGA Q50 device (TA Instruments) at a heating rate of 10 °C.min^{-1} under a nitrogen flow of 60 mL.min^{-1} for all tests. Dynamic Mechanical Analyses (DMA) were carried out with DMA 850 (TA Instruments) in parallel plate compression mode using a temperature sweep at a heating rate of 3 °C.min^{-1} from approximately −130 °C to 200 °C and a frequency of 1 Hz with an amplitude of 10 μm. The samples were 10 mm diameter and roughly 6 mm-thick. Dynamic Rheological Analyses (DRA) were performed with a MCR 302 rheometer (Anton Paar) in parallel plate shearing mode using: a) a strain amplitude sweep from 0.001 % to 100 % shear strain at room temperature and a frequency of 1 Hz; b) a frequency sweep from 0.1 rad.s^{-1} to 200 rad.s^{-1} of angular frequency ω at room temperature and a shear strain of 1 % and 0.01 %. The samples were 25 mm in width and roughly 1 mm-thick. This MCR 302 rheometer (Anton Paar) in parallel plate was also used in temperature ramp mode at 1 Hz and 1 % strain using a heating rate of 3 °C.min^{-1} from 30 °C to 360 °C. The samples were 8 mm in width and 1 mm-thick. Electrical conductivity measurements were performed on a high-resistance meter (6517B, Keithley) for the non-conductive samples and on a digital multimeter (DMM 7510, Keithley) for the

Chem. Eur. J. **2023**, e202301791 (9 of 11)

© 2023 Wiley-VCH GmbH

Chemistry–A European Journal

Research Article
doi.org/10.1002/chem.202301791

Chemistry
Europe
European Chemical
Societies Publishing

conductive CNT based samples. The resins samples (25 mm in diameter and roughly 1 mm-thick) were then placed on a circular interdigitated electrode pattern (Figure S3) and then tested at room temperature.

Modelling

Materials Studio 7.0 package was used to generate and build the PH-PDMS model systems. Initially, structures were established at a relatively low density ($0.4 \, \mathrm{g.cm^{-3}}$) and subsequently equilibrated in the NVT ensemble at 500 K for 5 ns. This was followed by an NPT simulation at 500 K for 20 ns and an additional 20 ns at 300 K, leading to the formation of a dense equilibrated phase. The simulations were performed using the LAMMPS package and the OPLS-AA forcefield.[93] Atomic charges were determined using the iterative Gasteiger method.[94] The van der Waals interactions were modeled using Lennard-Jones (12-6) with a cutoff distance of 1.2 nm. The electrostatic interactions were calculated using the Particle-Particle Particle-Mesh (PPPM) method with an accuracy value of $1.0e^{-4}$.

Supporting Information

Frequency-sweep DRA curves (Figures S1 and S2); set-up of the electrical measurements (Figure S3).

Conflict of Interests

The authors declare no conflict of interest.

Data Availability Statement

The data that support the findings of this study are available from the corresponding author upon reasonable request.

[1] Y. Zang, F. Zhang, C. A. Di, D. Zhu, *Mater. Horiz.* **2015**, *2*, 140–156.

[2] J. Li, L. Fang, B. Sun, X. Li, S. H. Kang, *J. Electrochem. Soc.* **2020**, *167*, 37561.

[3] M. Amjadi, K.-U. Kyung, I. Park, M. Sitti, *Adv. Funct. Mater.* **2016**, *26*, 1678–1698.

[4] F. Xu, X. Li, Y. Shi, L. Li, W. Wang, L. He, R. Liu, *Micromachines* **2018**, *9*, 1–17.

[5] O. Kanoun, A. Bouhamed, R. Ramalingame, J. R. Bautista-Quijano, D. Rajendran, A. Al-Hamry, *Sensors* **2021**, *21*, 341.

[6] R. B. Mishra, N. El-Atab, A. M. Hussain, M. M. Hussain, *Adv. Mater. Technol.* **2021**, *6*, 2001023.

[7] O. Kanoun, C. Müller, A. Benchirouf, A. Sanli, A. Bouhamed, A. Al-Hamry, L. Bu, in *Nanotechnol. Opt. Sensors* (Ed.: M. Aliofkhazraei), One Central Press (OCP), **2014**, pp. 148–183.

[8] O. Kanoun, R. Ramalingame, A. Al-Hamry, A. Bouhamed, J. R. Bautista-Quijano, D. Rejendran, in *2020 17th Int. Multi-Conference Syst. Signals Devices*, **2020**, pp. 1–6.

[9] A. M. Almassri, W. Z. Wan Hasan, S. A. Ahmad, A. J. Ishak, A. M. Ghazali, D. N. Talib, C. Wada, *J. Sensors* **2015**, *2015*, 846487.

[10] J. Li, R. Bao, J. Tao, Y. Peng, C. Pan, *J. Mater. Chem. C* **2018**, *6*, 11878–11892.

[11] X. Wang, J. Yu, Y. Cui, W. Li, *Sensors Actuators A Phys.* **2021**, *330*, 112838.

[12] J. Zhang, Y. Zhang, Y. Li, P. Wang, *Polym. Rev.* **2022**, *62*, 65–94.

[13] A. C. Katageri, B. Sheeparamatti, *Int. J. Eng. Res. Technol.* **2015**, *V4*, 665–671.

[14] W. Chen, X. Yan, *J. Mater. Sci. Technol.* **2020**, *43*, 175–188.

[15] M. T. Chorsi, E. J. Curry, H. T. Chorsi, R. Das, J. Baroody, P. K. Purohit, H. Ilies, T. D. Nguyen, *Adv. Mater.* **2019**, *31*, 1802084.

[16] M. K. Mohammed, A. Al-Nafiey, G. Al-Dahash, *Nano Biomed. Eng.* **2021**, *13*, 27–35.

[17] R. Li, Q. Zhou, Y. Bi, S. Cao, X. Xia, A. Yang, S. Li, X. Xiao, *Sensors Actuators A Phys.* **2021**, *321*, 112425.

[18] K.-H. Ha, H. Huh, Z. Li, N. Lu, *ACS Nano* **2022**, *16*, 3442–3448.

[19] M. Cao, J. Su, S. Fan, H. Qiu, D. Su, L. Li, *Chem. Eng. J.* **2021**, *406*, 126777.

[20] J. He, Y. Zhang, R. Zhou, L. Meng, T. Chen, W. Mai, C. Pan, *J. Mater.* **2020**, *6*, 86–101.

[21] J.-H. Pu, X.-J. Zha, M. Zhao, S. Li, R.-Y. Bao, Z.-Y. Liu, B.-H. Xie, M.-B. Yang, Z. Guo, W. Yang, *Nanoscale* **2018**, *10*, 2191–2198.

[22] M. Martin-Gallego, M. M. Bernal, M. Hernandez, R. Verdejo, M. A. Lopez-Manchado, *Eur. Polym. J.* **2013**, *49*, 1347–1353.

[23] S. Han, Q. Meng, S. Araby, T. Liu, M. Demiral, *Composites Part A* **2019**, *120*, 116–126.

[24] J. Lee, M. Lim, J. Yoon, M. S. Kim, B. Choi, D. M. Kim, D. H. Kim, I. Park, S.-J. Choi, *ACS Appl. Mater. Interfaces* **2017**, *9*, 26279–26285.

[25] M. L. Hammock, A. Chortos, B. C.-K. Tee, J. B.-H. Tok, Z. Bao, *Adv. Mater.* **2013**, *25*, 5997–6038.

[26] R. Ariati, F. Sales, A. Souza, R. A. Lima, J. Ribeiro, *Polymers (Basel).* **2021**, *13*, DOI 10.3390/polym13234258.

[27] I. Teixeira, I. Castro, V. Carvalho, C. Rodrigues, A. Souza, R. Lima, S. Teixeira, J. Ribeiro, *AIMS Mater. Sci.* **2021**, *8*, 952–973.

[28] I. Miranda, A. Souza, P. Sousa, J. Ribeiro, E. M. S. Castanheira, R. Lima, G. Minas, *J. Funct. Biomater.* **2021**, *13*, 2.

[29] L.-H. Cai, T. E. Kodger, R. E. Guerra, A. F. Pegoraro, M. Rubinstein, D. A. Weitz, *Adv. Mater.* **2015**, *27*, 5132–5140.

[30] D. Qi, K. Zhang, G. Tian, B. Jiang, Y. Huang, *Adv. Mater.* **2021**, *33*, 2003155.

[31] S. C. Shit, P. Shah, *Natl. Acad. Sci. Lett.* **2013**, *36*, 355–365.

[32] C. Robeyns, L. Picard, F. Ganachaud, *Prog. Org. Coat.* **2018**, *125*, 287–315.

[33] F. Y. Shih, B. R. Harkness, G. B. Gardner, J. S. Alger, M. R. Cummings, J. L. Princing, H. Meynen, H. A. Nguyen, W. W. Flack, in *Fifth Int. Conf. OnElectronic Packag. Technol. Proceedings, 2003. ICEPT2003.*, **2003**, pp. 316–320.

[34] H. Cong, T. Pan, *Adv. Funct. Mater.* **2008**, *18*, 1912–1921.

[35] U. J. Ana, G. W. Critchlow, K. M. Ford, N. R. Godfrey, D. B. Grandy, M. A. Spence, *Int. J. Adhes. Adhes.* **2010**, *30*, 781–788.

[36] H. Ishida, in (Eds.: H. Ishida, T. B. T.-H. of B. R. Agag), Elsevier, Amsterdam, **2011**, pp. 3–81.

[37] H. Ishida, Y. Rodriguez, *J. Appl. Polym. Sci.* **1995**, *58*, 1751–1760.

[38] H. Puozzo, S. Saiev, L. Bonnaud, J. De Winter, R. Lazzaroni, D. Beljonne, *Macromolecules* **2022**, *55*, 10831–10841.

[39] C. Zúñiga, L. Bonnaud, G. Lligadas, J. C. Ronda, M. Galià, V. Cádiz, P. Dubois, *J. Mater. Chem. A* **2014**, *2*, 6814–6822.

[40] L. Dumas, L. Bonnaud, M. Olivier, M. Poorteman, P. Dubois, *Eur. Polym. J.* **2014**, *58*, 218–225.

Chemistry–A European Journal

Research Article
doi.org/10.1002/chem.202301791

Chemistry Europe
European Chemical
Societies Publishing

[41] L. Dumas, L. Bonnaud, P. Dubois, in (Eds.: H. Ishida, P. B. T.-A. and E. P. S. and T. Froimowicz), Elsevier, Amsterdam, **2017**, pp. 767–800.

[42] S. Saiev, L. Bonnaud, L. Dumas, T. Zhang, P. Dubois, D. Beljonne, R. Lazzaroni, *ACS Appl. Mater. & Interfaces* **2018**, *10*, 26669–26677.

[43] S. Saiev, L. Bonnaud, C. Zúñiga, P. Dubois, D. Beljonne, J. C. Ronda, V. Cadiz, R. Lazzaroni, *Polym. Chem.* **2019**, *10*, 5251–5264.

[44] A. Beigbeder, M. Linares, M. Devalckenaere, P. Degée, M. Claes, D. Beljonne, R. Lazzaroni, P. Dubois, *Adv. Mater.* **2008**, *20*, 1003–1007.

[45] L. Bonnaud, L. Dumas, I. M. Murariu, M. Raimondo, S. Chirico, L. Guadagno, P. Longo, A. Mariconda, P. Dubois, *Proc. Eng. Against Fail.* **2015**, 1–7.

[46] M. Raimondo, C. Naddeo, L. Vertuccio, L. Bonnaud, P. Dubois, W. H. Binder, A. Sorrentino, L. Guadagno, *Nanotechnology* **2020**, *31*, 225708.

[47] K. Mojsiewicz-Pieńkowska, M. Jamrógiewicz, K. Szymkowska, D. Krenczkowska, *Front. Pharmacol.* **2016**, *7*, 132.

[48] X. Su, S. Song, C. Zhang, J. Huang, Y. Liu, M. Run, Y. Wu, *J. Appl. Polym. Sci.* **2016**, *133*, 44121.

[49] L. Liu, F. Wang, X. Wang, Y. Zhu, H. Qi, *Polym. Eng. Sci.* **2023**, *63*, 281–294.

[50] Y.-L. Liu, C.-W. Hsu, C.-I. Chou, *J. Polym. Sci. Part A* **2007**, *45*, 1007–1015.

[51] T. Takeichi, T. Kano, T. Agag, T. Kawauchi, N. Furukawa, *J. Polym. Sci. Part A* **2010**, *48*, 5945–5952.

[52] H. Li, J. Xu, K. Zeng, Y. Li, C. Z. G. Li, *High Perform. Polym.* **2019**, *32*, 268–275.

[53] H.-W. Lee, Y.-L. Liu, *J. Appl. Polym. Sci.* **2022**, *139*, e52605.

[54] R. Yang, B. Hao, L. Sun, K. Zhang, *J. Appl. Polym. Sci.* **2021**, *138*, 49792.

[55] A. Forchetti Casarino, M. E. Taverna, A. Candia, M. E. Spontón, G. R. Palmese, J. La Scala, D. A. Estenoz, *Polym. Adv. Technol.* **2023**, *34*, 840–854.

[56] B. Kiskan, B. Aydogan, Y. Yagci, *J. Polym. Sci. Part A* **2009**, *47*, 804–811.

[57] B. Aydogan, D. Sureka, B. Kiskan, Y. Yagci, *J. Polym. Sci. Part A* **2010**, *48*, 5156–5162.

[58] R. Sasi Kumar, N. Padmanathan, M. Alagar, *New J. Chem.* **2015**, *39*, 3995–4008.

[59] J. Xu, H. Li, K. Zeng, G. Li, X. Zhao, C. Zhao, *Thermochim. Acta* **2019**, *671*, 119–126.

[60] R. Sasi Kumar, M. Ariraman, M. Alagar, *RSC Adv.* **2015**, *5*, 40798–40806.

[61] P. Sharma, L. Nebhani, *Polymer* **2020**, *199*, 122549.

[62] J. Li, Z. Shen, H. Li, L. Xu, H. Song, G. Guan, G. Liu, *J. Appl. Polym. Sci.* **2019**, *136*, 47882.

[63] K. Zhang, X. Yu, S.-W. Kuo, *Polym. Chem.* **2019**, *10*, 2387–2396.

[64] C.-H. Lin, W.-B. Chen, W.-T. Whang, C.-H. Chen, *Polymers (Basel).* **2020**, *12*, DOI 10.3390/polym12112510.

[65] H. Li, C. Long, K. Zeng, Y. Li, C. Zhao, D. Xiang, Y. Wu, B. Wang, Z. Sun, Y. Que, *High Perform. Polym.* **2022**, *34*, 759–767.

[66] C.-Y. Hsieh, W.-C. Su, C.-S. Wu, L.-K. Lin, K.-Y. Hsu, Y.-L. Liu, *Polymer* **2013**, *54*, 2945–2951.

[67] W. Li, J. Chu, L. Heng, T. Wei, J. Gu, K. Xi, X. Jia, *Polymer* **2013**, *54*, 4909–4922.

[68] K.-C. Chen, H.-T. Li, W.-B. Chen, C.-H. Liao, K.-W. Sun, F.-C. Chang, *Polym. Int.* **2011**, *60*, 436–442.

[69] K.-C. Chen, H.-T. Li, S.-C. Huang, W.-B. Chen, K.-W. Sun, F.-C. Chang, *Polym. Int.* **2011**, *60*, 1089–1096.

[70] Z. Lu, W. Feng, X. Kang, J. Wang, H. Xu, Y. Wang, B. Liu, X. Fang, T. Ding, *Polym. Adv. Technol.* **2019**, *30*, 2686–2694.

[71] L. Wang, S. Zheng, *Polymer* **2010**, *51*, 1124–1132.

[72] C. Birsen Buldum, S. Gulyuz, Y. Yagci, B. Kiskan, *Eur. Polym. J.* **2022**, *174*, 111329.

[73] L. Liu, F. Wang, Y. Zhu, H. Qi, *High Perform. Polym.* **2022**, *35*, 251–263.

[74] V. Selvaraj, T. R. Raghavarshini, M. Alagar, *J. Polym. Environ.* **2019**, *27*, 2682–2696.

[75] M. Yuan, X. Lu, Y. Zhao, S.-W. Kuo, Z. Xin, *Polymer* **2022**, *245*, 124572.

[76] X. Ning, H. Ishida, *J. Polym. Sci. Part A* **1994**, *32*, 1121–1129.

[77] L. Liu, X. Han, W. Hu, B. Zhao, A. Fan, *Polym. Eng. Sci.* **2017**, *57*, 1127–1135.

[78] L. Han, D. Iguchi, P. Gil, T. R. Heyl, V. M. Sedwick, C. R. Arza, S. Ohashi, D. J. Lacks, H. Ishida, *J. Phys. Chem. A* **2017**, *121*, 6269–6282.

[79] L. Bonnaud, B. Chollet, L. Dumas, A. A. M. Peru, A. L. Flourat, F. Allais, P. Dubois, *Macromol. Chem. Phys.* **2019**, *220*, 1800312.

[80] Z. Wen, L. Bonnaud, R. Mincheva, P. Dubois, J.-M. Raquez, *Materials (Basel).* **2021**, *14*, 440.

[81] L. Zhang, M. Wang, J. Wu, *eXPRESS Polym. Lett.* **2016**, *10*, 617–626.

[82] S. Shukla, B. Lochab, *Polymer* **2016**, *99*, 684–694.

[83] A. Sudo, L.-C. Du, S. Hirayama, T. Endo, *J. Polym. Sci. Part A* **2010**, *48*, 2777–2782.

[84] M. Chapartegui, N. Markaide, S. Florez, C. Elizetxea, M. Fernandez, A. Santamaría, *Compos. Sci. Technol.* **2010**, *70*, 879–884.

[85] Q. Zhang, F. Fang, X. Zhao, Y. Li, M. Zhu, D. Chen, *J. Phys. Chem. B* **2008**, *112*, 12606–12611.

[86] H. Ishida, D. J. Allen, *Polymer* **1996**, *37*, 4487–4495.

[87] S. I. Kundalwal, A. Rathi, *J. Mech. Behav. Mater.* **2020**, *29*, 77–85.

[88] C.-L. Wu, H.-C. Lin, J.-S. Hsu, M.-C. Yip, W. Fang, *Thin Solid Films* **2009**, *517*, 4895–4901.

[89] K. T. S. Kong, M. Mariatti, A. A. Rashid, J. J. C. Busfield, *Polym. Bull.* **2012**, *69*, 937–953.

[90] S. S. Hassouneh, L. Yu, A. L. Skov, A. E. Daugaard, *J. Appl. Polym. Sci.* **2017**, *134*, 44767.

[91] L. R. Viannie, N. R. Banapurmath, M. E. M. Soudagar, A. V. Nandi, N. Hossain, A. Shellikeri, V. Kaulgud, M. A. Mujtaba, S. A. Khan, M. Asif, *J. Environ. Chem. Eng.* **2021**, *9*, 106550.

[92] Z. Brunovska, J. P. Liu, H. Ishida, *Macromol. Chem. Phys.* **1999**, *200*, 1745–1752.

[93] W. L. Jorgensen, D. S. Maxwell, J. Tirado-Rives, *J. Am. Chem. Soc.* **1996**, *118*, 11225–11236.

[94] J. Gasteiger, M. Marsili, *Tetrahedron* **1980**, *36*, 3219–3228.

RESEARCH ARTICLE

Our study focuses on preparing benzoxazine-terminated poly(dimethylsiloxane) (PH-PDMS) and developing elastomeric nanocomposites by incorporating multi-walled carbon nanotubes (MWCNTs). Through thermally curing, these nanocomposites demonstrate excellent electrical conductivity and mechanical stability, attributed to favorable MWCNT-matrix interactions which enable efficient dispersion of MWCNTs. These findings highlight the potential of these materials for pressure-sensing applications.
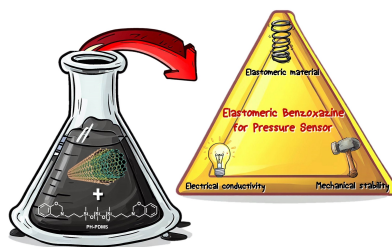
Dr. H. Puozzo, Dr. S. Saiev, Dr. L. Bonnaud*, Prof. Dr. D. Beljonne*, Prof. Dr. R. Lazzaroni*

1 – 12

Integrating Benzoxazine-PDMS 3D Networks with Carbon Nanotubes for flexible Pressure Sensors

SPACE RESERVED FOR IMAGE AND LINK

Share your work on social media! *Chemistry - A European Journal* has added Twitter as a means to promote your article. Twitter is an online microblogging service that enables its users to send and read short messages and media, known as tweets. Please check the pre-written tweet in the galley proofs for accuracy. If you, your team, or institution have a Twitter account, please include its handle @username. Please use hashtags only for the most important keywords, such as #catalysis, #nanoparticles, or #proteindesign. The ToC picture and a link to your article will be added automatically, so the **tweet text must not exceed 250 characters**. This tweet will be posted on the journal's Twitter account (follow us @ChemEurJ) upon publication of your article in its final form. We recommend you to re-tweet it to alert more researchers about your publication, or to point it out to your institution's social media team.

ORCID (Open Researcher and Contributor ID)

Please check that the ORCID identifiers listed below are correct. We encourage all authors to provide an ORCID identifier for each coauthor. ORCID is a registry that provides researchers with a unique digital identifier. Some funding agencies recommend or even require the inclusion of ORCID IDs in all published articles, and authors should consult their funding agency guidelines for details. Registration is easy and free; for further information, see http://orcid.org/.

Dr. Hugo Puozzo
Dr. Shamil Saiev
Dr. Leïla Bonnaud
Prof. Dr. David Beljonne
Prof. Dr. Roberto Lazzaroni http://orcid.org/0000-0002-6334-4068